Nonlinear behavior of structural and luminescent properties in $Gd(Nb_xTa_{1-x})O_4$ mixed crystals

Olesia Voloshyna[a], Oleg Sidletskiy[a], Dmitry Spassky[b], Iaroslav Gerasymov[a], Ivo Romet[c], Andrey Belsky[d]

[a] Institute for scintillation materials NAS of Ukraine, 60 Lenin av., Kharkiv 61001, Ukraine;

[b] Skobeltsyn Institute of Nuclear Physics, Moscow State University, Leninskie Gory 1, bld. 2, Moscow, 119991, Russia;

[c] Institute of Physics, University of Tartu, W. Ostwaldi Str.1, 50411, Tartu, Estonia;

[d] Université Lyon, Université Claude Bernard Lyon 1, CNRS, Institut Lumiere Matière, F-69622, Villeurbanne, France.

Corresponding author: lvoloshina@isma.kharkov.ua (O.V. Voloshyna)

Abstract

Ceramic samples of gadolinium tantalo-niobate mixed crystals were obtained by the solid-state technique. The dependence of luminescence properties on the Nb/Ta ratio in the $Gd(Nb_xTa_{1-x})O_4$ system is studied in the 5 – 450 K temperature range, including thermostimulated luminescence curves in the series of solid solutions. The relation of nonlinear behavior of light output with x variation to non-homogeneous distribution of Nb and Ta in solid solutions is discussed.

Keywords

Mixed crystals, luminescence, lattice parameters, clusterization, $GdNbO_4$, $GdTaO_4$

1. Introduction

Currently the fast and heavy crystals are needed for the application in scintillation detectors [1]. Scintillators with activator emission are commonly used for such purposes. However, crystals with intrinsic emission are preferable in case of cryogenic scintillators when activator emission becomes inefficient due to the self-trapping of charge carriers by the host lattice at low temperature [2,3]. $REAO_4$ compounds (A = Ta or Nb) demonstrate intrinsic luminescence attributed to the emission of regular TaO_6 - and NbO_6 – groups and defect groups NbO_5V_O and TaO_5V_O (V_O – oxygen vacancy) [4-7]. The brightest luminescence was observed in the rare earth niobates [4]. At the same time, rare-earth tantalates demonstrate an extremely high density and stopping power [8]. Engineering of mixed compositions by Nb^{5+}/Ta^{5+} substitution can be a tool to enhance the light yield and other scintillation parameters by analogy with many other mixed systems studied recently [9-16]. It was shown that the tendency to light yield increase in mixed crystals is linked to the spatial distribution of substituted atoms in solid solutions which, in turn, determines their electronic properties. Basing on luminescence properties study it was suggested that spatial inhomogeneities of electronic structure affect the dynamics of relaxation, recombination, and localization of free carriers [9,10,12]. This approach was confirmed by the dependence of light yield improvement in mixed crystals on ionic radii difference between the substituted atoms [17]. Meanwhile, the improvement of charge carriers transport efficiency to activator and a huge light yield increase was linked to enveloping of the electron trap levels in the conduction band in some mixed crystals [18-21].

Light output and decay times of the tantalo-niobates [$RE(Nb_xTa_{1-x})O_4$] strongly depends on the Ta/Nb ratio [22]. Light output of $Gd(Ta_{1-x}Nb_x)O_4$ at room temperature shows about gradual

increase with Nb content. The fast decay component with the τ varied within 5 – 93 ns range is accompanied by the slow component for all compositions except $Gd(Ta_{0.8}Nb_{0.2})O_4$. Recently, single crystals with the latter composition were successfully grown by the Czochralski technique [23]. In this scintillator the high density of 8.37 g/cm^3 is combined with the light output of 1400 ph./MeV and very fast luminescence with the main decay time of 17 ns.

The present study focuses on structural and luminescence properties of $Gd(Ta_{1-x}Nb_x)O_4$ (x = 0 ÷ 1), including thermostimulated luminescence (TSL) curves analysis. We also discuss the evidences of clusterization in these solid solutions basing on dependences of various physical properties on the Ta/Nb ratio.

2. Experimental

2.1. Raw materials

Ceramic samples of gadolinium tantalate-based compounds with varying Nb content from 0 to 100 at.% were obtained by the solid-state synthesis (details are described in [22]). Gd_2O_3 (Stanford Materials Co, USA) and Ta_2O_5, Nb_2O_5 (Lanhit, Russia) with purity not less than 4N were used as starting materials. XRD data on the obtained samples indicate that all the $Gd(Nb_xTa_{1-x})O_4$ samples crystallize in the M-fergusonite structure (space group I 2/a) with the main phase content of 95-97 wt.% [22]. After solid-state synthesis the pellets were prepared for the study of luminescent and scintillation properties by polishing of their surfaces to the identical surface roughness providing the same light collection conditions from all of the samples.

2.2. Characterization techniques

The luminescence spectra under excitation with synchrotron radiation (SR) with excitation energy 22 eV have been obtained at the branch-line FINEST at MAX-lab, Lund [24]. The spectra were measured using ARC Spectra Pro 300i monochromator equipped with Hamamatsu H6240-01

photon counting head in the temperature range 5 – 300 K. TSL curves were studied in the temperature range T = 100 – 550 K. Samples were mounted into LINKAM THMS600 Stage. The spectra were registered using a Shamrock 500i spectrograph equipped with a Newton EMCCD DU970P. The heating rate at TSL measurements was 10 K/min.

The luminescence excitation spectra were measured at 300 K in the wavelength range 200-350 nm using the deuterium Heraeus D 200 VUV lamp as an excitation source. The McPherson Model 234/302 primary monochromator was used for the selection of excitation wavelength. The luminescence was registered using the Shamrock 303i (Andor Technology) monochromator equipped with the Hamamatsu H8259 photon counting head.

3. Experimental results

3.1 Cell parameters

Deviations of lattice constants from the Vegard's law were noticed previously in many mixed crystals, e.g. in MgO-FeO, MgO-$LiFeO_2$ [25], and CdF_2-PbF_2 systems [26], and attributed to the formation of inhomogeneities (clusters) enriched with one of substituted atoms. In $Gd(Nb_xTa_{1-x})O_4$ the *b* cell parameter and the elementary cell volume determined recently in [22] demonstrate similar positive deviations at x = 0.2 - 0.6 (Fig. 1).

[Fig. 1]

3.2 Luminescence properties

The luminescence spectra of $Gd(Nb_xTa_{1-x})O_4$ at T = 300 K are presented in Fig.2a. The excitation energy of SR was 22 eV providing interband electron transitions. The excitation energy is high enough to model the processes which takes place in a scintillator at the final stages of energy relaxation including the photon multiplication, thermalization of hot charge carriers and their

migration to the emission centers. The photon multiplication process starts at $E_{ex} \geq 2E_g$. According to [27] the band gap energies for gadolinium tantalate and niobate are 5.4 eV and 4.6 eV, respectively. Therefore, the excitation energy exceeds the bandgap values of the studied samples by the factor of 4.1-4.8. At $x \neq 0$ all the samples demonstrate a broad emission band with the maximum around 450 nm. It was shown previously [28] that emission in rare earth tantalo-niobates possesses the complex structure and consists of the short-wavelength band peaked at 415 nm and ascribed to the exciton-like emission at regular oxyanion complexes NbO_6, and the long-wavelength band peaked at 460 nm, which is connected with the point defects, in particular, oxygen vacancies (NbO_5V_O-group). Consequently, the $Gd(Nb_xTa_{1-x})O_4$ emission observed in this work at room temperature can be ascribed to the defect-related emission.

[Fig. 2]

The intrinsic emission is not manifested, probably, due to the thermal quenching, or due to efficient transfer from regular to defect states [4]. The broad but weak emission band in $GdTaO_4$ (Fig. 2a, curve 1) is red-shifted and linked to TaO_5V_O-group emission [28]. The several sharp peaks at 380, 420, 440, 490, 550, 590 and 610 nm observed for the latter are related to emission of Eu^{3+} and Tb^{3+} impurities. The peak at 310 nm linked with the emission of the cell-forming Gd^{3+} ion and is most pronounced for the $GdTaO_4$. Less intensity of this band for Nb-containing samples should be linked with more efficient energy transfer from Gd^{3+} ion to NbO_5V_O-group.

The excitation spectra of the emission at 460 nm are presented in Fig.3.

[Fig. 3]

The peak at 295 – 305 nm is located below the bandgap and is connected with the direct excitation of the defect center. The low-energy shift of the bandgap with **x** is revealed in the corresponding shift of the peak's maximum. The rise of intensity at shorter wavelengths relates to the energy transfer from the region of fundamental absorption edge. The rise is not sharp and it does not allow to trace the bandgap shift. In might be related to the defect origin of the emission center, which is excited via consecutive capture of electrons and holes (recombination type of energy transfer to emission centers, see e.g [29]).

The luminescence spectra of $Gd(Nb_xTa_{1-x})O_4$ ($x\neq0$) at T = 5 K (Fig. 2b) are similar to those at T = 300 K with maximum around 450 nm. Therefore, exciton-like emission of regular oxyanion complexes NbO_6 are not observed for gadolinium tantaloniobates at low temperature as well. For $GdTaO_4$ the broad band with maximum around 395 nm was detected (Fig. 2b, curve 1). In [4] the intrinsic luminescence of $GdTaO_4$ at T=77 K was supposed similar to the defect-related emission in $YTaO_4$ with maximum around 400-420 nm. Thus, the band observed in the present study (395 nm) can be ascribed to intrinsic emission in $GdTaO_4$. Note, this band is completely absent i) on the $Gd(Nb_xTa_{1-x})O_4$ ($x\neq0$) luminescence spectra at T = 5 K confirming the efficient transfer from regular TaO_6-groups to defect states and ii) on the $GdTaO_4$ luminescence spectrum at T = 300 K confirming the thermal quenching of intrinsic luminescence.

3.3 Thermostimulated luminescence

Thermostimulated luminescence curves (Fig. 4a) provide an information on traps modification in the solid solution. Up to five peaks can be seen at the TSL curves of $Gd(Ta_{1-x}Nb_x)O_4$. Two TSL peaks are inherent for all samples – the weak one at 120-160 K and the most intensive one at 230 -270 K. Therefore, these peaks relate to the defects, which origin does not connected with Nb or Ta cations. We tentatively attribute them to oxygen vacancies. The shift of these peaks to lower temperatures with increase of x corresponds to the decrease of activation energy of the corresponding trap. The tendency is attributed to the decrease of the mean band gap

from $GdTaO_4$ to $GdNbO_4$. It is worth noting that the width of TSL peaks depends on x value as well. The FWHM of the most prominent TSL peak at ~250 K depends non-linearly on x with the maximum at x = 0.4 (Fig. 4b).

[Fig. 4]

3.4 Light output.

The efficient transfer from host to emission centers in solid solutions might cause a significant increase of light output for intermediate x values of $Gd(Nb_xTa_{1-x})O_4$ at T = 16 K (Fig. 5a). The similar effect of light output enhancement has been previously observed in some mixed oxide crystals at room temperature [9-16]. Here we demonstrate that the effect can be also observed at low temperatures as well. Therefore, it can be utilized for the tailoring of cryogenic scintillators with the improved scintillation performance. The linear dependence of light output at T = 300 K is connected with the contribution of some additional processes to the light output formation, e.g. of emission thermal quenching, which is observed for all studied crystals (Fig.5b). The temperature dependence of the luminescence intensity can't be approximated by the Mott law for any of the studied sample. Under 22 eV excitation the separated electrons and holes are created in the conduction and valence band. Besides the radiative relaxation of electron-hole pairs at NbO_5V_O emission center the separated change carriers can also migrate to some other non-radiative relaxation centers or to be captured by the traps. The presence of traps in $Gd(Nb_xTa_{1-x})O_4$ is confirmed by the TSL curves presented in Fig.3. Relaxation of charge carriers via these competitive to emission channels influences the temperature dependence of emission intensity.

[Fig. 5]

4 Discussion

The detailed consideration of dependences of physical properties of $Gd(Nb_xTa_{1-x})O_4$ mixed crystals reveals some evidences of spatial inhomogeneity in them, namely:

- loosening of the lattice at x=0.2-0.4 means that Ta and Nb are uniformly distributed in lattice in these compositions;
- the broadening of the main TSL peak for intermediate compositions indicates the wider distribution of activation energy of the trap due to the bandgap spatial fluctuations caused by the inhomogeneity in the solid solution;
- finally, the non-linearity for the light output at 16 K and the linear dependence at 300 K supports the hypothesis on correlation between spatial inhomogeneities in scintillation crystals and shortening of the carrier separation length in them [9,10,12].

As charge carriers in crystals are situated in periodic electrostatic field formed by crystal lattice ions, in a mixed crystal the amplitude of crystal field oscillations should increase in case of formation of clusters enriched by one of the substituted ions. The bandgap difference (ΔE_g) between the mixed crystal constituents is also matters, because clusters limit electron and hole separation at $\Delta E_g >> kT$. This is the case of the considered system where ΔE_g between $GdTaO_4$ and $GdNbO_4$ is 0.8 eV [27]). As kT is by 19 times higher at 300 K compared to that at 16 K, the limitation of electron and hole separation at 16 K causes the increase of the light output in the intermediated compositions, while at 300 K no evidence of carrier separation length limitation is observed (possibly, due to thermal quenching of luminescence). Note that the cluster size must be large enough to influence the carrier separation length, which in dielectric crystals is from 1 nm up to several tens of nm depending on the relaxation speed on the stage of phonon scattering.

At the moment few data are available to distinguish the role of preparation procedure itself (solid state synthesis from powders) in cluster formation. According to the specifications, powder particle size of starting oxides used for the solid-state synthesis of ceramic samples is less than $6.6 \cdot 10^{-5}$ m (250 mesh). Since solid-state synthesis is a heterogeneous reaction, interaction took place on the particle surface. For correct description of the synthesis mechanism one should take

into account the diffusion mobility of the interacting ions. The diffusion mobility inversely proportional to the melting point (m.p.) of the compound [30] and increases in the row Gd (Gd_2O_3 m.p. 2420 °C) < Ta (Ta_2O_5 m.p. 1872 °C) < Nb (Nb_2O_5 m.p. 1512 °C). Obviously, the interaction took place on the Gd_2O_3 particle surface while Ta_2O_5 and Nb_2O_5 were supplied to the interaction surface by diffusion. However, at the moment there is no available data on size of formed tantaloniobate grains, as well as Ta- or Nb- enriched clusters in them.

Instead, the nanoscale clusters in the considered system can be formed by intrinsic properties of the solid solution. Note, the band gap in GTO 5.4 eV and GNO 4.6 eV [27] differs by 0.8 eV. Numerical simulation in a model mixed system $A_{1-x}B_xC$ [31] shows that sufficiently large E_g spatial fluctuations with the amplitude of up to 0.8 ΔE_g are formed in the case of affinity between AA or BB atoms, e.g. a high probability to occupy neighboring positions in the lattice by atoms of the same sort. Meanwhile, at high AA or BB affinity the cluster size reaches hundreds of elementary cell volumes, while it is negligible in the case of AB affinity. At random distribution of A and B atoms the calculated E_g and cluster size are intermediate between the AA (BB) and AB affinity cases and the bandgap spatial fluctuations amplitude reaches $0.35\Delta E_g$. Meanwhile, physical or chemical factors affecting such affinity were not discussed in [31].

Considering the chemical affinity as the capability of interaction between atoms or compounds, the Nb-Ta affinity (energy of chemical bond formation between Ta and Nb) in $Gd(Nb_xTa_{1-x})O_4$ is low because of similar electronegativities of 1.5 in Ta and 1.6 in Nb by the Pauling scale [32]. According to the empirical Pauling formula for the evaluation of Δ_{Ta-Nb} as the energy of chemical bond formation between Ta and Nb relatively to the hypothetical covalent bond

$$0.208*(\Delta_{Ta-Nb})^{1/2}=\left|\chi_{Ta}-\chi_{Nb}\right|$$

(χ_{Ta} and χ_{Nb} are electronegativities of Ta and Nb, respectively), Δ_{Ta-Nb} is around 30 kJ/mol. Accounting for the average chemical bond energy of several hundreds of kJ/mol, the Δ_{Ta-Nb} value is negligible. As no Nb-Nb or Ta-Ta chemical interaction can be expected too, random distribution of Nb and Ta in $Gd(Nb_xTa_{1-x})O_4$ is preferable, unless some unknown factors exist affecting the Nb-Ta

affinity, or the affinity between the same sort of atoms. However, the maximum deviations of cell parameters and light output are shifted from x = 0.5 (expected maximum deviation at random Ta/Nb distribution) to x = 0.2 – 0.4 pointing at some Nb-Nb affinity and formation of Nb-enriched clusters [31]. Nevertheless, deeper structural studies (e.g. EXAFS) are needed to obtain a direct confirmation of clusters formation, and other possible causes of Nb-Nb affinity should be analyzed.

Conclusions

The analysis of structure and luminescence properties of $Gd(Nb_xTa_{1-x})O_4$ mixed crystals on Nb/Ta ratio indicates an inuniformity of substitutional ions distribution over the crystal lattice resulting in the spatial band gap energy fluctuations. Meanwhile, the presence of positive light output deviations just at low temperatures indicates that amplitudes of these fluctuations are higher than the *kT* energy at ~16 K and significantly smaller compared to E_g = 0.8 eV between $GdTaO_4$ and $GdNbO_4$. Despite no evidence of chemical affinity between Nb-Ta, or Nb-Nb (Ta-Ta) was found, the maximal deviations of lattice parameters, light output at 16 K, and FWHM of the strongest TSL peak from the linearity are observed at x = 0.2 – 0.6. This indicates a tendency to formation of Nb enriched clusters over the lattice in $Gd(Nb_xTa_{1-x})O_4$.

Funding

The work was partially supported by the Marie Skłodowska- Curie Research, Innovation Staff Exchange Project H2020-MSCA-RISE-2014 no. 644260 “INTELUM”. Financial support of Russian Ministry of Education and Science (Agreement 14.616.21.0006, Identification No RFMEFI61614X0006) is gratefully acknowledged. This work was supported by grant RFBR 15-02-07825-a and by institutional research funding IUT (IUT02-26) of the Estonian Ministry of Education and Research.

References

[1] M. Martinez, C. Cuesta, E. Garcia, C. Ginestra, A. Ortiz de Solórzano, Y. Ortigoza, C. Pobes, J. Puimedón, T. Rolón, M. L. Sarsa, J. A. Villar, N. Coron, J. Gironnet, J. Leblanc, P. de Marcillac, T. Redon, L. Torres, P. Veber, M. Velázquez, Development of scintillating bolometers for dark matter searches, Journal of Modern Physics: Conference Series 23 (2013) 324–328.

[2] S.S. Gridin, A.N. Belsky, N.V. Shiran, A.V. Gektin, Channels of energy losses and relaxation in CsI:A scintillators (A=Tl ,In). IEEE T Nucl. Sci. 61 (2014) 246-251.

[3] S. Gridin, A. Belsky, C. Dujardin, A. Gektin, N. Shiran, A. Vasil'ev, Kinetic model of energy relaxation in CsI: A (A= Tl and In) scintillators, J. Phys. Chem. C, 119 (2015) 20578-2059.

[4] G. Blasse, A. Brill, Luminescence phenomena in compounds with fergusonite structure, J. Lumin. 3 (1970) 109-131.

[5] L.H. Brixner, H.-Y. Chen, On the structural and luminescent properties of the $M'LnTaO_4$ rare earth tantalates. J. Electrochem. Soc.: Solid-state science and technology, 130 (1983) 2435-2443.

[6] W.J. Schipper, M.F. Hoogendorp, G. Blasse, The luminescence and X-ray storage properties of Pr^{3+} and Ce^{3+} in $YNbO_4$ and M'-$YTaO_4$. J. Alloy. Compd., 202 (1993) 283-287.

[7] O. Voloshyna, S.V. Neicheva, N.G. Starzhinskiy, I.M. Zeny, S.S. Gridin, V.N. Baumer, O.Ts. Sidletskiy, Luminescent and scintillation properties of orthotantalates with common formulae $RETaO_4$ (RE = Y, Sc, La, Lu and Gd), Mater. Sci. Eng. B 178 (2013) 1491-1496.

[8] M.Z. Su, W. Zhao, Rare earth ions in advanced X-ray imaging materials, in: G. Liu, B. Jacquier, (Eds), Spectroscopic properties of rare earths in optical materials, Berlin: Springer Heidelberg. 2005. p. 500-529.

[9] A.G. Petrosyan, K.L. Ovanesyan, G.O. Shirinyan, T.I. Butaeva, C. Pedrini, C. Dujardin, A. Belsky, Growth and light yield performance of dense Ce^{3+}-doped $(Lu,Y)AlO_3$ solid solution crystals, J. Cryst. Growth 211 (2000) 252-256.

[10] A.N. Belsky, E. Auffray, P. Lecoq, C. Dujardin, N. Garnier, H. Canibano, C. Pedrini, A.G. Petrosyan, Progress in the development of $LuAlO_3$-based scintillators, IEEE T Nucl. Sci. 48 (2001) 1095-1100.

[11] O. Sakthong, W. Chewpraditkul, C. Wanarak, J. Pejchal, K. Kamada, A. Yoshikawa, G.P. Pazzi, M. Nikl, Luminescence and scintillation characteristics of $Gd_3Al_2Ga_3O_{12}:Ce^{3+}$ scintillators, Opt. Mater. 36 (2013) 568-571.

[12] O. Sidletskiy, A. Belsky, A. Gektin, S. Neicheva, D. Kurtsev, V. Kononets, C. Dujardin, Kh. Lebbou, O. Zelenskaya, V. Tarasov, K. Belikov, B. Grinyov, Structure–property correlations in a Ce-doped $(Lu, Gd)_2SiO_5$: Ce scintillator, Cryst. Growth Des. 12, (2012) 4411-4416.

[13] O. Sidletskiy, V. Kononets, Kh. Lebbou, S. Neicheva, O. Voloshina, V. Bondar, V. Baumer, K. Belikov, A. Gektin, B. Grinyov, M.-F. Joubert, Structure and scintillation yield of Ce-doped Al–Ga substituted yttrium garnet, Mater. Res. Bull. 47 (2012) 3249-3252.

[14] K. Kamada, T. Endo, K. Tsutumi, T. Yanagida, Y. Fujimoto, A. Fukabori, A. Yoshikawa, J. Pejchal, M. Nikl, Composition engineering in cerium-doped $(Lu, Gd)_3(Ga, Al)_5O_{12}$ single crystal scintillators, Cryst. Growth Des., 11 (2011) 4484-4490.

[15] V.S. Levushkina, V.V. Mikhailin, D.A. Spassky, B.I. Zadneprovski, M.S. Tret'yakova, Luminescence properties of solid solutions of borates doped with rare-earth ions, Phys. Solid State 56 (2014) 2247-2258.

[16] D. Spassky, S. Omelkov, H. Mägi, V. Mikhailin, A. Vasil'ev, N. Krutyak, I. Tupitsyna, A. Dubovik, A. Yakubovskaya, A. Belsky, Energy transfer in solid solutions $Zn_xMg_{1-x}WO_4$, Opt. Mater. 36 (2014) 1660-1664.

[17] O. Sidletskiy, A. Gektin, A. Belsky, Light-yield improvement trends in mixed scintillation crystals, Phys. Status Solidi A 211 (2014) 2384-2387.

[18] M. Fasoli, A. Vedda, M. Nikl, C. Jiang, B. P. Uberuaga, D. A. Andersson, K. J. McClellan, C. R. Stanek, Band-gap engineering for removing shallow traps in rare-earth $Lu_3Al_5O_{12}$ garnet scintillators using Ga^{3+} doping, Phys. Rev. B84 (2011) 081102(R).

[19] Yu.V. Zorenko, Mechanism of dissipation of the excitation energy in garnet oxides doped with rare-earth ions with 4*f*-5*d* transitions, Opt. Spectrosc. 88 (2000) 551-553.

[20] M. Nikl, A. Vedda, V. V. Laguta, Energy transfer and storage processes in scintillators: The role and nature of defects, Radiat. Meas. 42 (2007) 509-514.

[21] W. Drozdowski, K. Brylew, M.E. Witkowski, A.J. Wojtowicz, P. Solarz, K. Kamada, A. Yoshikawa, Studies of light yield as a function of temperature and low temperature thermoluminescence of $Gd_3Al_2Ga_3O_{12}$:Ce scintillator crystals, Opt. Mater. 36 (2014) 1665–1669.

[22] O.V. Voloshyna, I.A. Boiaryntseva, V.N. Baumer, A.I. Ivanov, M.V. Korjik, O.Ts. Sidletskiy, New, dense, and fast scintillators based on rare-earth tantalo-niobates. Nucl. Instrum. Meth. A 764 (2014) 227-231.

[23] O. Voloshyna, I. Gerasymov, O. Sidletskiy, D. Kurtsev, T. Gorbacheva, K. Hubenko, I. Boiaryntseva, A. Ivanov, D. Spassky, S. Omelkov, A. Belsky, Fast ultradense $GdTa_{1-x}Nb_xO_4$ scintillator crystals, Opt. Mater. 66 (2017) 332-337.

[24] T. Balasubramanian, B. N. Jensen, S. Urpelainen, B. Sommarin, U. Johansson, M. Huttula, R. Sankari, E. Nõmmiste, S. Aksela, H. Aksela, R. Nyholm, The normal incidence monochromator beamline I3 on MAX III, AIP Conf. Proc. 1234 (2010) 661- 664.

[25] G. A. Waychunas, W.A. Dollase, C.R. Ross II, Short-range order measurements in MgO-FeO and MgO-LiFeO, solid solutions by DLS simulation-assisted EXAFS analysis. Am. Mineral. 79 (1994) 274-288.

[26] M.A.P. Silva, Y. Messaddeq, V. Briois, M. Poulain, F. Villain, S. J. L. Ribeiro, Structural studies on lead–cadmium fluoride solid solutions, Solid State Ionics 147 (2002) 135–139.

[27] A.H. Krumpel, P. Boutinaud, E. van der Kolk, P. Dorenbos, Charge transfer transitions in the transition metal oxides ABO4:Ln3+ and APO4:Ln3+ (A=La, Gd, Y, Lu, Sc; B=V, Nb, Ta; Ln=lanthanide). J. Lumin., 130 (2010) 1357–1365.

[28] O. Voloshyna, Ia. Boiaryntseva, D. Spassky, O. Sidletskiy, Luminescence properties of the yttrium and gadolinium tantalo-niobates, Sol. St. Phen. 230 (2015) 172-177.

[29] N.R.Krutyak, V.V.Mikhailin, A.N.Vasil'ev, D.A.Spassky, I.A.Tupitsyna, A.M.Dubovik, E.N.Galashov, V.N.Shlegel, A.N.Belsky, The features of energy transfer to the emission centers in $ZnWO_4$ and $ZnWO_4$:Mo. J. Lumin., 144 (2013) 105-111.

[30] A.R. West, Solid state chemistry and its applications. second ed. John Wiley and Sons, Chichester-New York-Brisbane-Toronto-Singapore. 2014.

[31] A. Belsky, A. Gektin, S. Gridin, A.N. Vasiliev, Electronic and optical properties of scintillators based on mixed ionic crystals, pp. 63-84 in: Korzhik M. and Gektin A. (Ed.) Engineering of Scintillation Materials and Radiation Technologies, Springer, 2017, 339 p.

[32] N.N. Greenwood, E. Earnshaw, Chemistry of the elements. second ed. Butterworth-Heinemann. 1997.

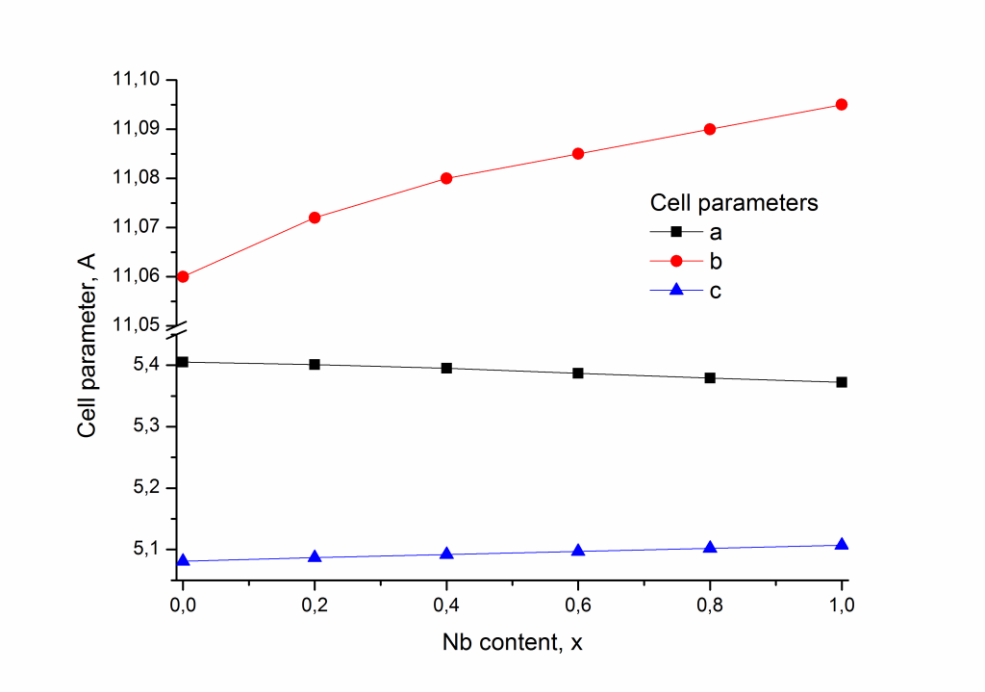

a

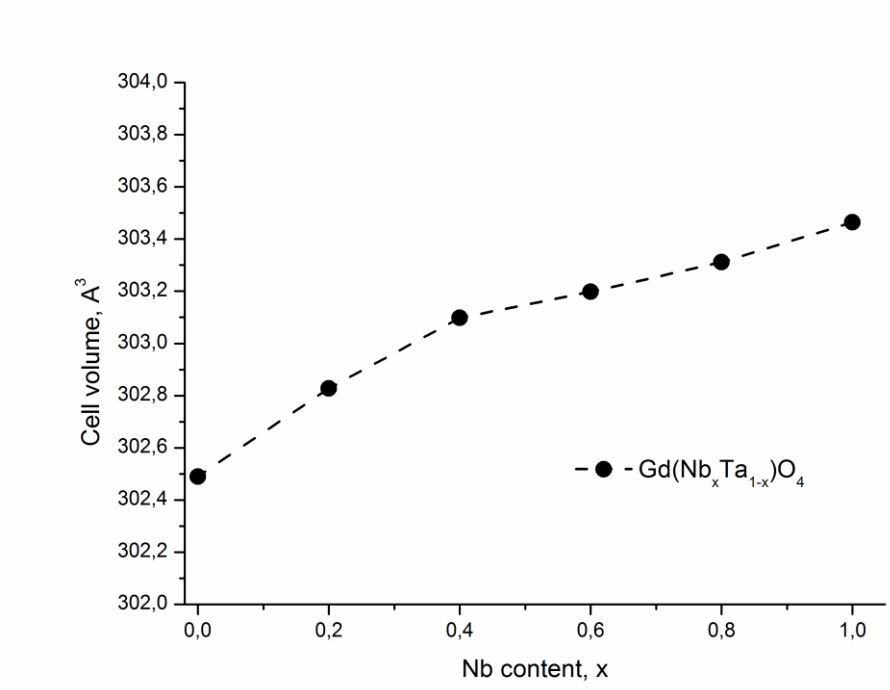

b

Fig. 1 Dependence of the cell parameters (a) and cell volume (b) on the x value for $Gd(Ta_{1-x}Nb_x)O_4$.

1

2

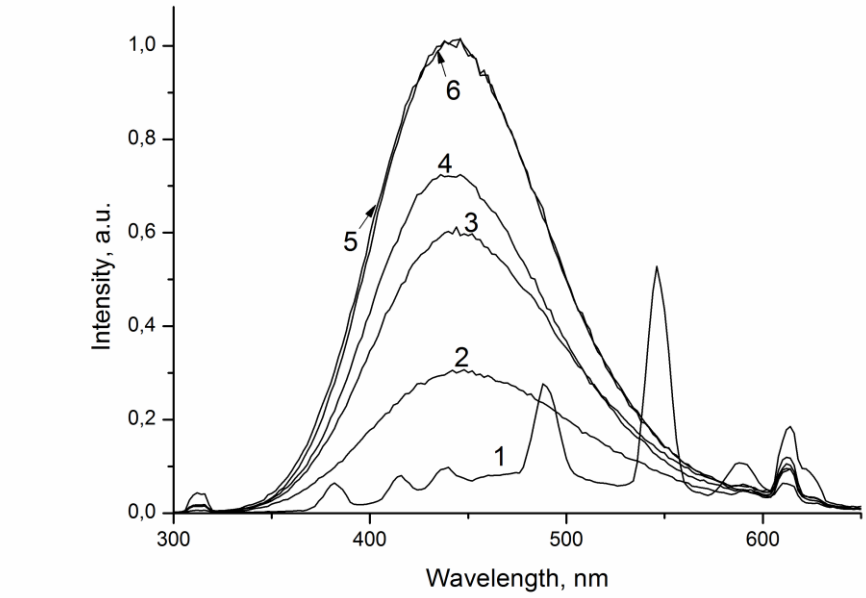

a

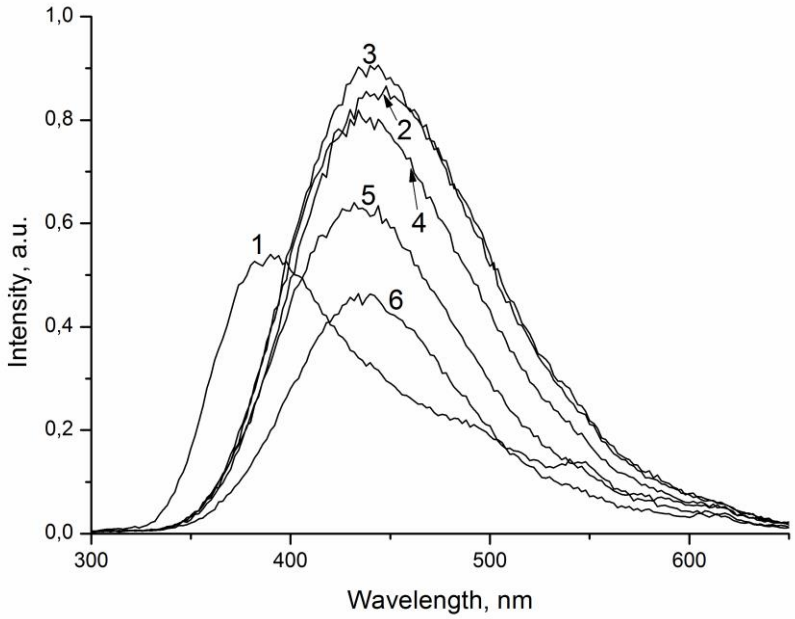

b

Fig. 2 Emission spectra of $Gd(Nb_xTa_{1-x})O_4$ (x=0 (1); x=0.2 (2); x=0.4 (2); x=0.6 (4); x=0.8 (5) and x=1 (6)) normalized by the maximum of the brightest curve under synchrotron radiation excitation, E_{ex} = 22 eV at T = 300 K (a) and T = 5 K (b).

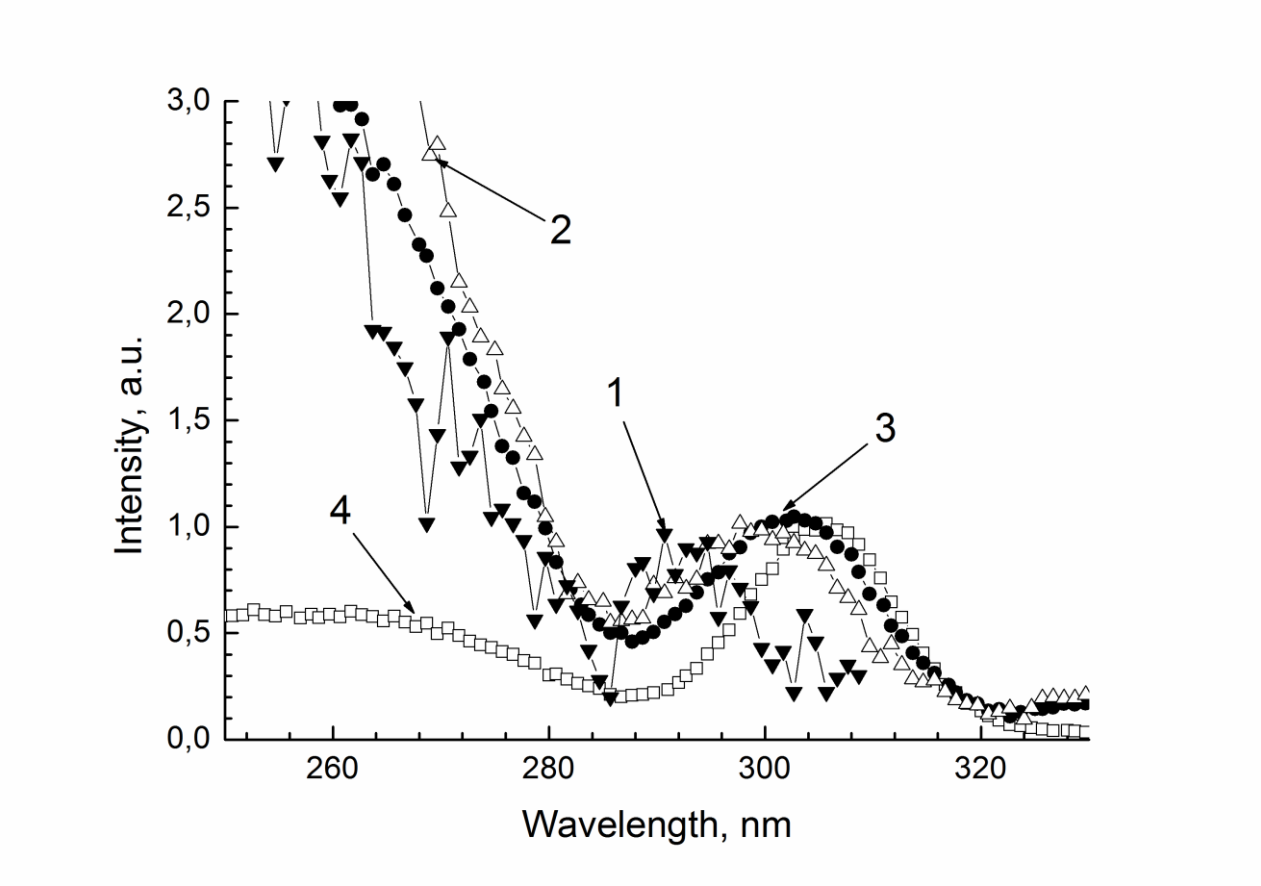

Fig. 3 Luminescence excitation spectra of $Gd(Nb_xTa_{1-x})O_4$ (x=0.2 (1); x=0.4 (2); x=0.6 (3) and x=0.8 (4)) at λ_{em} = 460 nm, T = 300 K

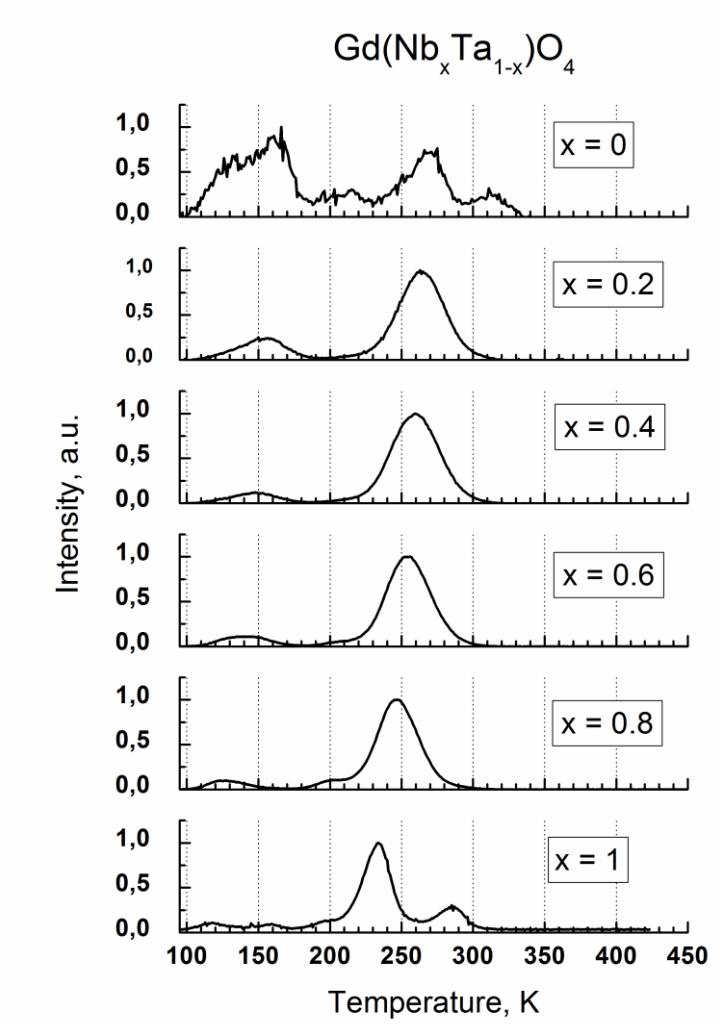

a

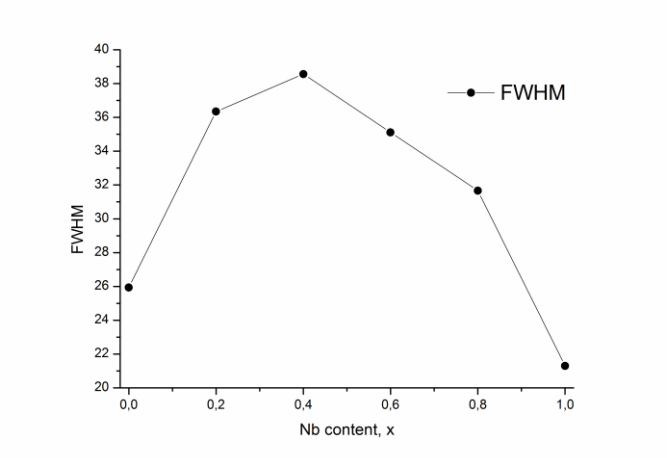

b

Fig. 4 TSL curves (a) and dependence of the ~250 K peak FWHM on the x value (b) in $Gd(Ta_{1-x}Nb_x)O_4$.

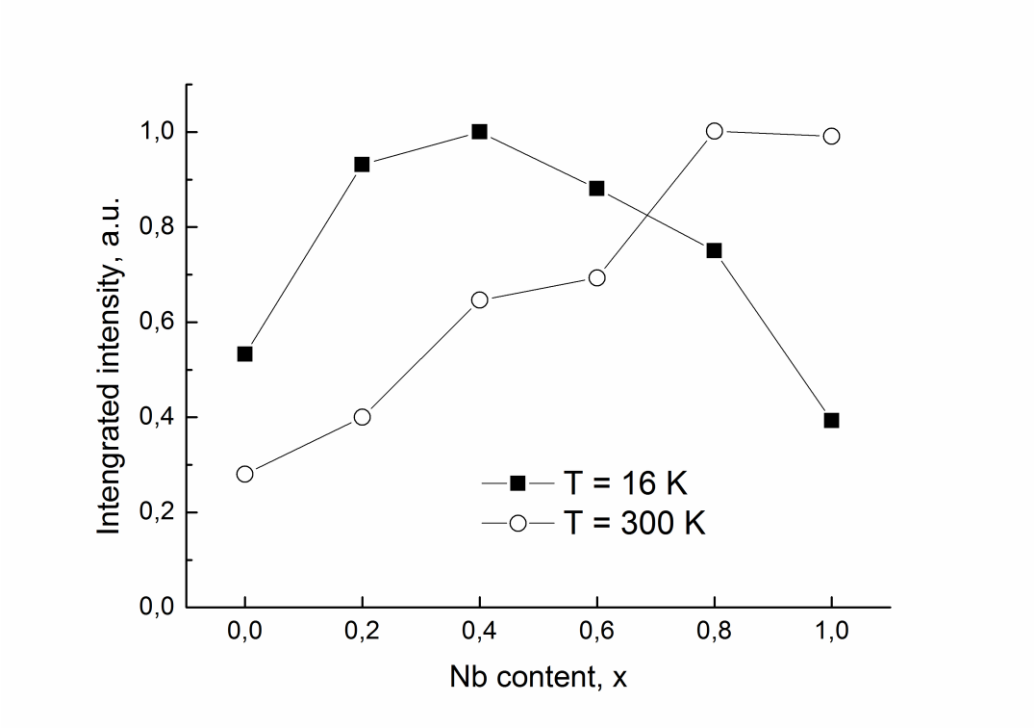

a

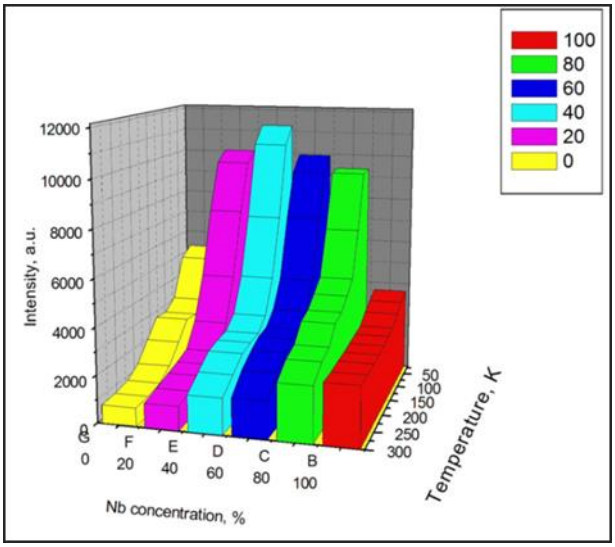

b

Fig. 5 Dependence of light output in $Gd(Nb_xTa_{1-x})O_4$ on x value: a – under SR excitation at temperatures 16 K and 300 K, b – temperature dependence of light output under SR excitation, E_{ex}=22 eV.